Future Cities and Environment
ISSN 2363-9075 Volume 12 (2026)

https://doi.org/10.70917/fce-2026-018

Article

Punching Shear Behavior of Polymer Nanocomposite Flat Slabs with Shear Reinforcement under Monotonic Loading

Saloma [1,*], Siti Aisyah Nurjannah [1], Arie Putra Usman [1], Anis Saggaff [1], Muhammad Irham Dhafin [1] and Mohammad Firdaus Abu Hashim [2,3]

[1] Civil Engineering Department, Faculty of Engineering, Universitas Sriwijaya, Indralaya, Ogan Ilir, 30662 Indonesia
[2] Center of Excellence Geopolymer and Green Technology (CEGeoGTech), Universiti Malaysia Perlis, Perlis 01000, Malaysia
[3] Faculty of Mechanical Engineering Technology, Universiti Malaysia Perlis, Kampus Tetap Pauh Putra, Perlis 02600, Malaysia
* Correspondence author: salomaunsri@gmail.com

Abstract: This study investigates the punching shear response of flat slabs made with polymer nanocomposite materials and different amounts of shear reinforcement under monotonic loading. Eight slab models were analyzed using three-dimensional finite element analysis, including both normal concrete and polymer nanocomposite slabs. The results show that adding shear reinforcement increases the load the slabs can carry and limits their deformation. In the polymer nanocomposite models, the ultimate load increased from 525 kN without shear reinforcement to 562.5 kN with Ø12 shear reinforcement, while the maximum deflection was reduced by up to 38.1%. Compared with the normal concrete models, the polymer nanocomposite slabs carried 45–55% higher loads and dissipated up to 238% more energy. The higher stiffness and shear resistance obtained with additional reinforcement were accompanied by a small reduction in ductility, indicating a stiffer response before failure. The stress contours also showed that larger shear reinforcement diameters spread the stress over a wider region and reduced the concentration around the column. Taken together, the results show that polymer nanocomposite materials can improve the punching shear response of flat slabs, particularly when combined with suitable shear reinforcement.

Keywords: Polymer nanocomposite; punching shear; shear reinforcement; stress contour

1. Introduction

The use of high-rise buildings has increased as infrastructure development continues in many areas. In these structures, flat slabs are commonly used because they do not require beams and can therefore provide a simpler floor layout, lower story height, and reduced structural weight. The main concern with this system is its susceptibility to punching shear near the column–slab connection, where the concentrated stresses can lead to a sudden local failure (Shatarat et al., 2022; Alnemrawi et al., 2024; Lima et al., 2021; Ismail et al., 2022). The failure usually develops through inclined cracks that form around the column, eventually producing a truncated cone-shaped failure surface (Hamoda et al., 2024; Qader et al., 2015; Panahi et al., 2022).

Punching shear failure is generally brittle and can occur with little warning, as the slab may fail without undergoing substantial deformation beforehand. This makes punching shear particularly dangerous because the failure can cause serious structural damage and, in severe cases, may trigger progressive collapse (Guo et al., 2023; Milligan et al., 2020; Baniya et al., 2020). Improving the punching shear resistance of flat slabs is still a challenge in structural design. One common solution is to add shear reinforcement around the column, such as stirrups or stud rails, so that the slab can carry a higher shear force. The slab geometry can also be changed by using a larger column or a drop panel, which provides more area for transferring the load near the column. Fiber-reinforced materials have also been studied, mainly because they contribute to crack control and post-cracking deformation. SCS composite systems provide another possible solution and have been investigated for their ability to improve the shear behavior of flat slabs and maintain structural integrity.

Shear reinforcement is a common way to improve the behavior of flat slabs around the column. Its role becomes important once cracks develop because the reinforcement can bridge the cracked region and help transfer tensile forces. Several studies have reported improved strength and deformation behavior when shear reinforcement is introduced in the critical region of the slab (Torabian et al., 2019; Inacio et al., 2015; Gouveia et al., 2018; Al-Rousan et al., 2023). The response of a slab under punching shear, however, cannot be explained by the reinforcement alone. The punching response of a slab is affected by more than the shear reinforcement itself. Concrete strength, longitudinal reinforcement, slab thickness, loading arrangement, and slab geometry can all influence the way the slab responds to punching shear (Oliveira et al., 2022; Eom et al., 2017; Raafat et al., 2021; Lapi et al., 2020).

In this study, the slab material is a polymer nanocomposite. In general, polymer nanocomposites are produced by incorporating nano-sized particles into a polymer matrix, and the resulting material can show properties that differ from those of the polymer alone. Previous work has reported their potential for strength, corrosion resistance, and thermal insulation (Septriansyah et al., 2021; Septriansyah et al., 2025). Their use in flat slab applications, particularly for punching shear, has received much less attention. This raises an important structural question: when the material changes, does the punching shear response change only because of its mechanical strength, or does the material also affect how stresses and cracks develop around the column. Flat slab models with polymer nanocomposite materials were studied under monotonic loading. Several shear reinforcement arrangements were considered to see how they affected the slab response, particularly around the column where punching failure was expected to develop. The load–deformation response was recorded throughout the analysis, together with the changes in cracking and the final failure pattern. The comparison also considered the shear reinforcement ratio, slab thickness, and material properties. These results were then used to examine how the slab behavior changed as loading progressed and how the damage developed before punching failure.

Most previous studies of punching shear have dealt with conventional reinforced concrete, fiber-reinforced concrete, high-strength concrete, or different forms of shear reinforcement. These studies have provided a substantial basis for understanding how to increase a slab's punching capacity. Less is known about what happens when the material itself is changed to a polymer nanocomposite. In particular, information remains limited on whether such a material affects the distribution of stresses around the column, the path and development of cracks, the progression of damage, and the loss of stiffness as loading continues. These aspects are important because an increase in peak load alone does not necessarily indicate a better punching shear response.

To investigate these effects, this study uses three-dimensional nonlinear finite element analysis to examine the interaction between the polymer nanocomposite material and the shear reinforcement. Rather than treating the material as a simple replacement for conventional concrete with a different compressive strength, the analysis considers its influence on the slab–column region response as loading progresses. The study's main contribution is therefore an examination of the relationship between material characteristics, reinforcement arrangement, stress transfer, and failure development in polymer nanocomposite flat slabs.

The study examines how the polymer nanocomposite material and shear reinforcement affect the punching response of the slab. It is expected that providing shear reinforcement in the polymer nanocomposite slabs will give the load another path to travel around the column and help limit the concentration of damage. The reinforcement arrangement and material properties are also expected to affect the way cracks develop and, consequently, the failure pattern. Another point of interest is the deformation response. A suitable reinforcement arrangement may help the slab retain its stiffness and continue to deform before punching failure occurs, which could also affect its ductility and energy dissipation.

2. Research significance

The work compares flat slabs made with conventional concrete and polymer nanocomposite materials, with different shear reinforcement arrangements considered under monotonic loading. The comparison is not limited to the maximum load. Changes in stiffness, deformation, cracking, and energy absorption are also examined to see whether the use of the polymer nanocomposite affects the way punching failure develops around the column.

A nonlinear three-dimensional finite element model is used to examine these differences under the same loading conditions. This makes it possible to compare the response of the two slab systems and to examine the changes in stress distribution and damage development. The results are intended to provide a better understanding of the punching behavior of polymer nanocomposite flat slabs and the role of shear reinforcement in their structural response.

3. Methodology

The flat slab model adopted in this study follows previous research (Ewees et al., 2024), as shown in Figures 1 and 2. The slab measures 1500 mm × 1500 mm and is reinforced with 16 Ø10 mm compression bars and 13 Ø12 mm tension bars. Various shear reinforcement configurations were considered (Table 1). The column has a 150 mm × 150 mm cross-section. Its longitudinal reinforcement consists of Ø12 mm bars at the outer regions and Ø10 mm bars at the center in a 4 × 4 arrangement. Transverse reinforcement comprises six Ø8 mm stirrups spaced at 50 mm. The materials used in this study consisted of normal concrete and polymer nanocomposite concrete. The mechanical properties of normal concrete were adopted from (Ewees et al., 2024), For the flat slab without shear reinforcement, the compressive strength was 36.18 MPa with an elastic modulus of 28,270.41 MPa, while the slab with shear reinforcement had a compressive strength of 34.93 MPa and an elastic modulus of 27,777.76 MPa. The polymer nanocomposite concrete properties were adopted from Septriansyah et al. (2021), with a compressive strength of 56.65 MPa and an elastic modulus of 35,375.1 MPa. The polymer nanocomposite incorporated nano-silica particles, which enhanced the mechanical properties through matrix densification, pore refinement, and improved interfacial bonding within the cementitious matrix.

The higher stiffness, crack resistance, and load transfer observed for the polymer nanocomposite were taken into account in the numerical model. The material was defined using a nonlinear concrete model, with the mechanical properties obtained from the experimental results. The model included both compressive and tensile behavior, as well as the stress–strain response of the material. Crack formation and the reduction in stiffness after cracking were also considered so that the model could represent the slab response under monotonic loading. The finite element simulations were carried out in ANSYS Workbench 2023 R1. SOLID65 elements were used to represent the concrete and polymer nanocomposite. These elements were selected to account for the nonlinear response of the material, including cracking and crushing. The reinforcing bars were modeled with LINK180 elements, while SOLID185 elements were used for the steel plates and supports. The material nonlinearity was defined using multilinear isotropic hardening, and the William–Warnke failure criterion was used to describe cracking in the concrete.

For the connection between the reinforcement and concrete, a perfect bond was assumed. This means that the reinforcement and the surrounding concrete were assumed to deform together, without relative movement at the interface. The assumption was made to keep the model manageable; however, it does not represent bond–slip that may occur in an actual slab. This may have an effect on the way cracks initiate and propagate, as well as on the transfer of shear forces near the column. Therefore, the possible influence of bond–slip is recognized as a limitation of the present model.

The load was applied incrementally so that the response of the slab could be followed as cracking and other nonlinear effects developed. The force and displacement convergence criteria available in the ANSYS solver were used to check the solution at each increment. Automatic time stepping was also applied, together with equilibrium iterations, to help the analysis follow the changes in stiffness during loading.The mesh size was checked before carrying out the main simulations. Several element sizes were compared to see whether further mesh refinement produced a meaningful change in the numerical response. A mesh size of 30 mm was finally used. This size gave a stable response without adding unnecessary computational time associated with a finer mesh. The model was then checked against the experimental results reported by Ewees et al. (2024). The comparison included the load–deflection response, ultimate load, deformation behavior, and punching failure pattern. The numerical results showed a similar trend to the experimental response, indicating that the model was suitable for the subsequent analysis of polymer nanocomposite flat slabs with different shear reinforcement arrangements.

Table 1. Variations of Shear Reinforcement in Flat Slabs.

Model	Tension Reinforcement	Compression Reinforcement	Shear Reinforcement	Concrete Type	Compressive Strength (MPa)
S0N	13 Ø 12	16 Ø 10	-	Normal concrete	36.18
S8N	13 Ø 12	16 Ø 10	Ø8 - 100	Normal concrete	34.93
S10N	13 Ø 12	16 Ø 10	Ø10 - 100	Normal concrete	34.93
S12N	13 Ø 12	16 Ø 10	Ø12 – 100	Normal concrete	34.93
S0P	13 Ø 12	16 Ø 10	-	Polymer nanocomposite	56.65
S8P	13 Ø 12	16 Ø 10	Ø8 – 100	Polymer nanocomposite	56.65
S10P	13 Ø 12	16 Ø 10	Ø10 – 100	Polymer nanocomposite	56.65
S12P	13 Ø 12	16 Ø 10	Ø12 - 100	Polymer nanocomposite	56.65

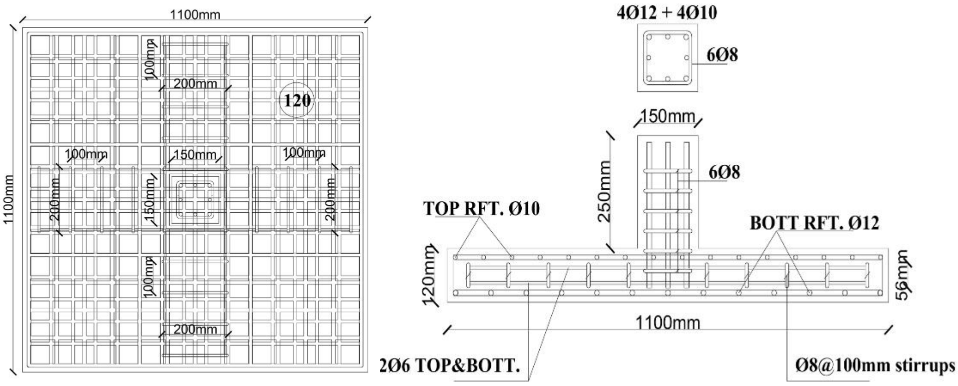

Figure 1. Flat slab model with shear reinforcement

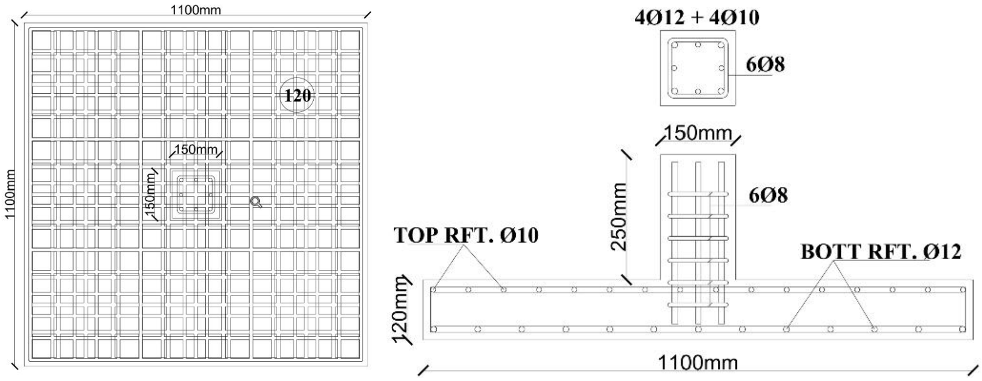

Figure 2. Flat slab model without shear reinforcement

The reinforcing steel properties were adopted from Ewees et al. (2024). The flat slab was modeled using plain reinforcing bars with Ø10 mm diameter as the top (compression) reinforcement and Ø12 mm as the bottom (tension) reinforcement. Shear reinforcement was varied to evaluate its influence on the structural response, using Ø8 mm (S8), Ø10 mm (S10), and Ø12 mm (S12) stirrups to represent different shear reinforcement ratios. The slabs were subjected to monotonic loading. The load was applied axially through the column and increased by 50 kN at each step until the model failed. As the load increased, the column transferred load to the surrounding slab, causing increasing slab deformation. The resulting load–deflection response was used to compare the behavior of the different reinforcement configurations. The slab–column system is the result of a three-dimensional finite element model. The geometry was first defined from the slab and column dimensions, with separate models prepared for cases with and without shear reinforcement. The material properties and element definitions were then assigned based on the adopted experimental data. The mesh was generated after the element types and model geometry had been defined. The final models were then used to simulate the slab response under the applied monotonic load. Figure 3 shows an example of the flat slab model.

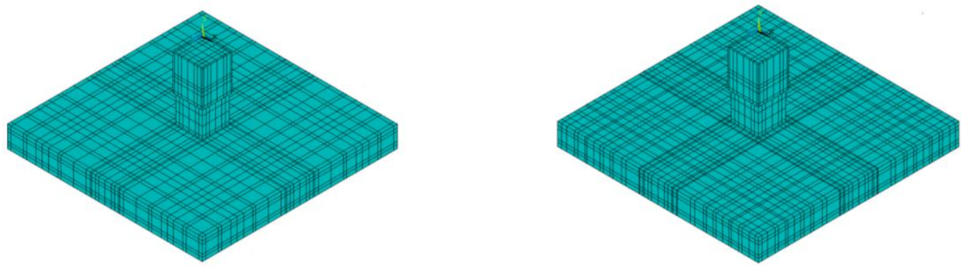

(a) (b)

Figure 3**.** Flat slab finite element model: **(a)** without shear reinforcement; **(b)** with shear reinforcement

4. Results and Discussion

4.1. Load–Deflection Relationship

The discussion considers how the material properties and shear reinforcement affect the punching response of the slabs. The changes in load transfer, stress distribution, damage development, stiffness, ductility, and energy absorption are examined together with the numerical results to understand the behavior around the slab–column connection. The load–deflection response is also used to follow the behavior of the slabs during loading. Deflection is plotted on the x-axis and the applied load on the y-axis, allowing the changes in stiffness and deformation to be observed as loading progresses.

The numerical response is compared with the experimental results reported by Ewees et al. (2024) for model validation. The comparison includes the load–deflection response and the maximum deflection obtained from the numerical and experimental results. A difference of less than 10% is considered acceptable. For a direct comparison, the numerical results are taken from nodes located at the same positions as the Linear Variable Differential Transducers (LVDTs) used in the experimental test. The validation results are then used as the basis for applying the model to the analysis of flat slabs with polymer nanocomposite materials and different shear reinforcement arrangements.

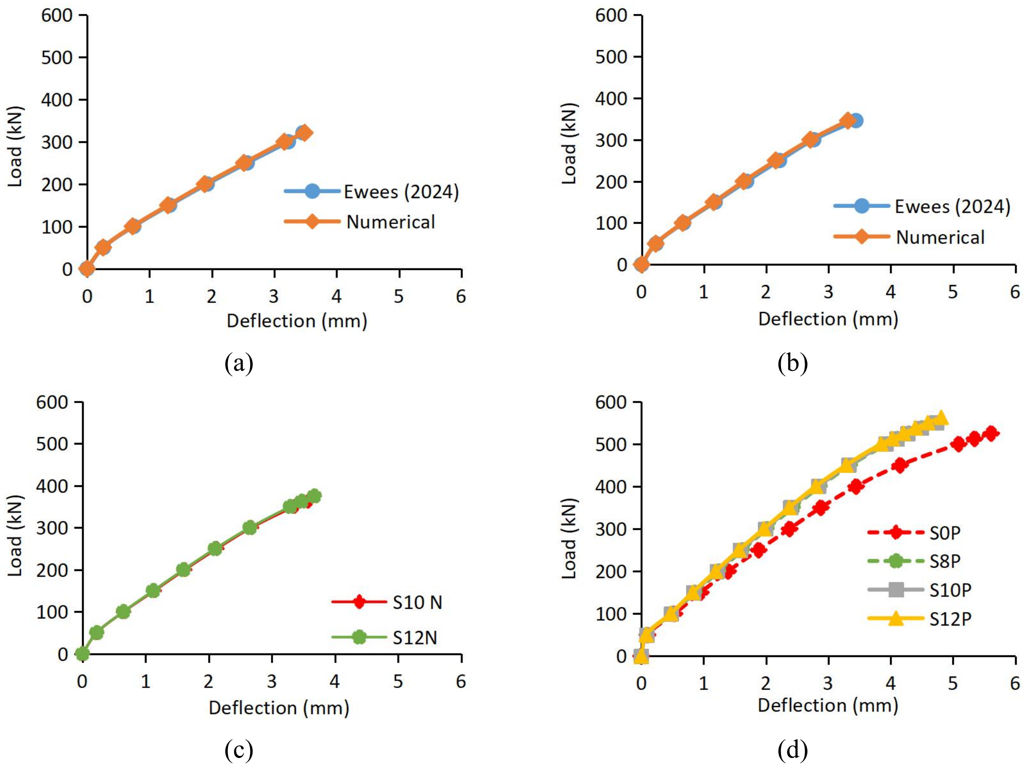

Figure 4**.** Load–deflection relationship for: (a) S0N model; (b) S8N model; (c) S10N and S12N; (d) polymer nanocomposite concrete

The load–deflection curves indicate that the unreinforced model (S0N) exhibits lower load-carrying capacity and greater deflection than the reinforced specimens (Figure 4(a)). In contrast, models with shear reinforcement (S8N, S10N, and S12N) demonstrate increased load capacity and reduced deflection, reflecting enhanced stiffness (Figures 4(b) and 4(c)). This behavior is attributed to shear reinforcement that facilitates stress transfer across cracks, delays crack propagation, and limits crack opening. Consequently, aggregate interlock and dowel action are improved, increasing resistance to punching shear. Validation results show deviations of 0.818% (S0N) and 3.703% (S8N), both within the acceptable limit (≤10%), confirming the reliability of the numerical model. Minor discrepancies are attributed to mesh discretization, boundary condition idealization, and experimental uncertainties.

For reinforced models S10N and S12N, increasing the diameter of shear reinforcement reduces deflection under identical loading (350 kN), indicating increased stiffness due to improved resistance to shear-induced tensile stresses and enhanced crack control (Schmidt et al., 2020; Isufi et al., 2021). In polymer nanocomposite slabs, the maximum load increases progressively from 525 kN (S0P) to 562.5 kN (S12P). The S0P model exhibits the largest deflection, whereas S12P achieves the highest load capacity (Figure 4(d)). A trend consistent with normal concrete is observed, where increasing reinforcement diameter enhances stiffness and reduces deflection.

The polymer nanocomposite slabs carried higher loads than the normal concrete slabs, but the difference cannot be explained by compressive strength and stiffness alone. The stress patterns around the slab–column connection also changed. In the polymer nanocomposite models, the stress was distributed over a wider region and the development of local damage occurred later as the load increased. The slabs were also able to retain their stiffness for a longer part of the loading process and continued to deform before the punching failure became dominant. The load capacity of the polymer nanocomposite slabs was about 45–55% higher than that of the normal concrete slabs. This difference is likely related to the combined effect of the material properties and the way the load was transferred around the column. Stress redistribution, damage development, and the amount of energy absorbed by the slab all contributed to the response observed in the numerical models. For validation, the numerical load–deflection curves and deformation response were compared with the experimental results. The model followed the main trend of the experimental curves and showed a similar failure response. The comparison gives reasonable confidence in the numerical model for the subsequent parametric analysis. However, the load–deflection response by itself does not explain the reason for the higher punching capacity. The stress distribution and damage pattern around the column provide additional information about how the polymer nanocomposite changed the punching shear response.

4.2. Stress contour of normal concrete flat slab

The stress contour results for normal concrete flat slabs are shown in Figures 5-8 indicate that stress concentrations primarily occur around the slab–column connection region due to concentrated load transfer, thereby identifying this area as critical for punching shear failure. The unreinforced model (S0N) exhibits a highly localized stress distribution, with a pronounced peak compressive stress around the column, indicating limited capacity for stress redistribution and greater susceptibility to punching shear failure. The maximum compressive stress reaches−112.742 N/mm², while the tensile stress remains relatively low (SMX = 1.19332 N/mm²), indicating a compression-dominated stress state.

Adding shear reinforcement changes the stress distribution around the slab–column connection. In S8N, the peak compressive stress increases, but the stress is spread over a wider region compared with S0N. The stirrups provide additional paths for shear transfer, while crack bridging, aggregate interlock, and dowel action also contribute to the load transfer. With the larger stirrup diameter in S10N, the stress field becomes wider and more evenly distributed, and the peak compressive stress is about 35.6% higher than in S0N. S12N shows a slightly different response, with a more uniform stress distribution around the connection even though its peak compressive stress is about 4.1% lower than that of S10N. This suggests that the larger stirrup diameter in S12N helps spread the applied load over a wider area rather than simply increasing the maximum stress at a particular location. Overall, increasing the shear reinforcement diameter reduces stress concentration and enhances punching shear resistance. Although localized stress peaks remain due to numerical discretization, the results consistently show improved structural behavior and greater load-carrying capacity as the shear reinforcement ratio increases (Ewees et al., 2024; Schmidt et al., 2020; Isufi et al., 2021).

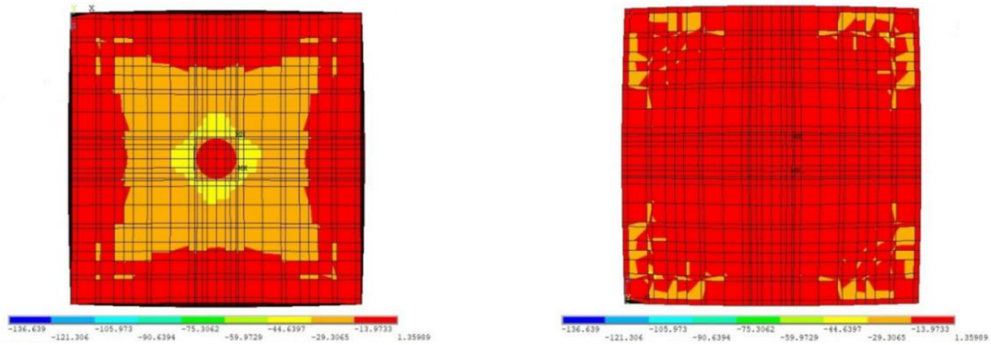

(a) (b)

Figure 5. Stress contour of the S0N flat slab model: (a) top view, (b) bottom view

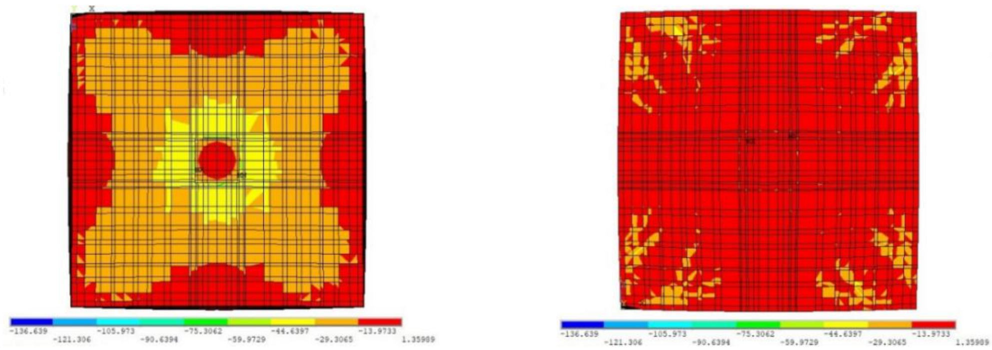

(a) (b)

Figure 6. Stress contour of the S8N flat slab model: (a) top view, (b) bottom view

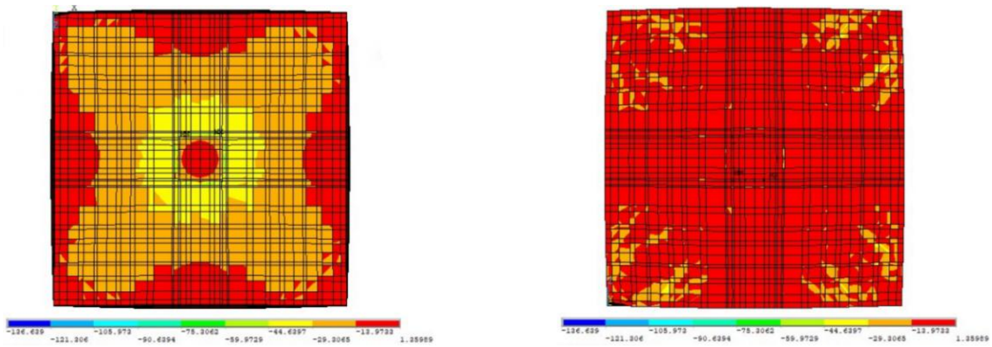

(a) (b)

Figure 7. Stress contour of the S10N flat slab model: (a) top view, (b) bottom view

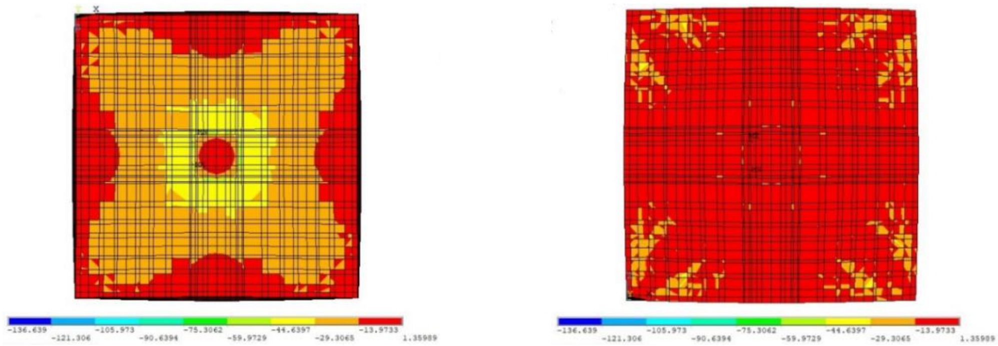

(a) (b)

Figure 8. Stress contour of the S12N flat slab model: (a) top view, (b) bottom view

4.3. Stress Contour of Polymer Nanocomposite Flat Slab

The stress contour distributions of polymer nanocomposite flat slabs for models S0P, S8P, S10P, and S12P are presented in Figures 9–12. The stress pattern becomes less concentrated around the column as the shear reinforcement diameter increases. In S0P, where no shear reinforcement is provided, the load is transferred mainly from the column directly into the slab. As a result, the highest compressive stresses are concentrated close to the column, ranging from 59.97 to 90.64 MPa. Tensile stresses are also present on the bottom surface of the slab, which corresponds to the region where cracking develops. After cracking, the concrete contributes less to tensile resistance, so the reinforcing bars take a larger part of the load. Adding Ø8 mm stirrups in S8P changes the stress pattern around the column. High stresses are still present, but they are spread over a wider region than in S0P. The stirrups provide an additional path for transferring shear across the cracked area. The change becomes more apparent in S10P, where the larger stirrup diameter produces a broader stress field around the column. The stress is distributed over a larger part of the slab instead of remaining concentrated in a small area. S12P shows a similar trend, with the stress field becoming more evenly distributed around the column. The highest stresses are still found near the column, which is expected for punching shear, but a greater part of the surrounding slab is involved in carrying the load. Thus, the difference between S10P and S12P cannot be judged only from their peak stress values; the distribution of stress across the slab is also important. The overall change from S0P to S12P suggests that the stirrups help transfer shear across the cracked region through mechanisms such as crack bridging, dowel action, and aggregate interlock (Ewees et al., 2024; Schmidt et al., 2020; Isufi et al., 2021). Some localized stress peaks remain in all models, which is expected near the column because of the high stress gradient and the finite element discretization.

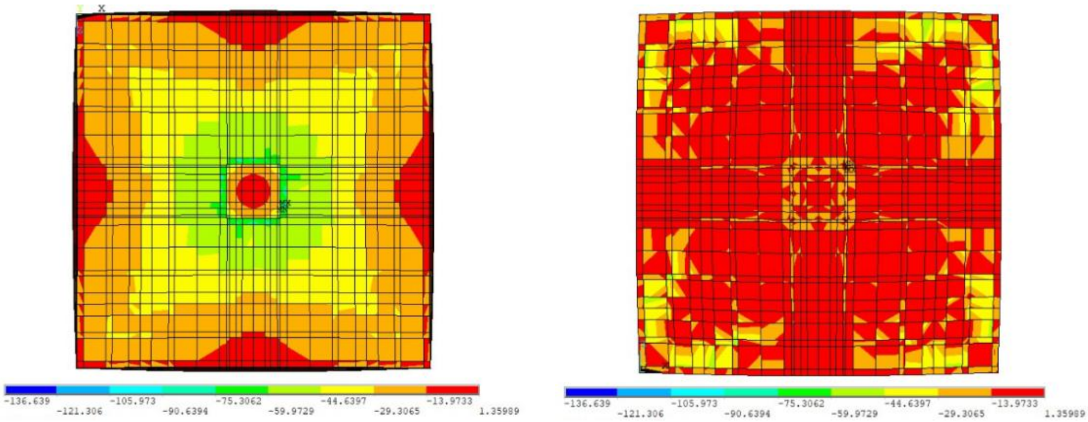

(a) (b)

Figure 9. Stress contour of the S0P flat slab model: (a) top view, (b) bottom view

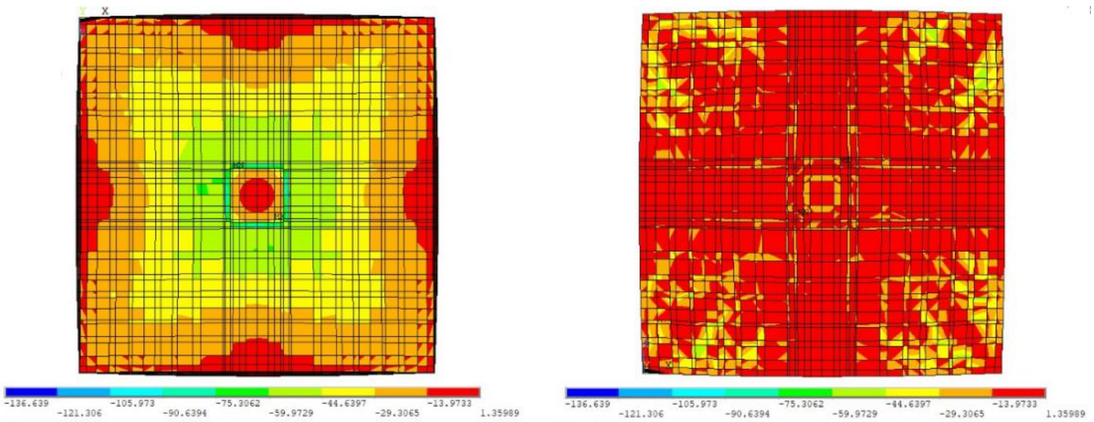

(a) (b)

Figure 10. Stress contour of the S8P flat slab model: (a) top view, (b) bottom view

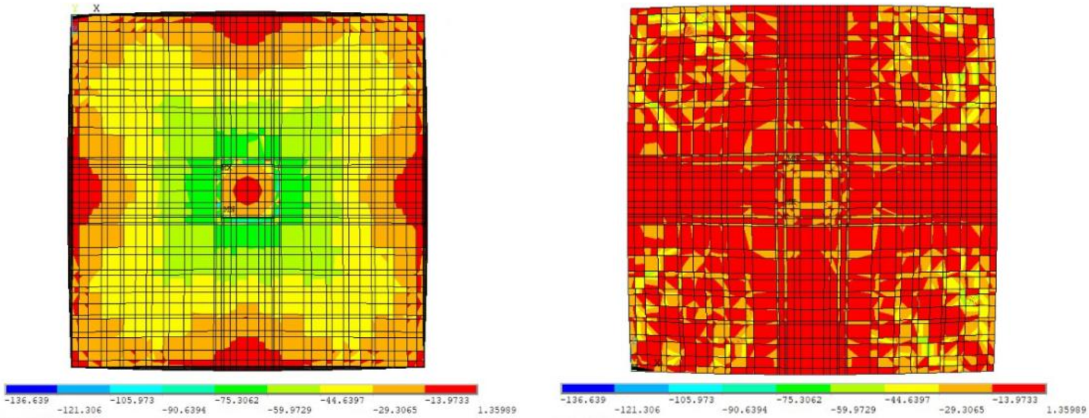

(a) (b)

Figure 11. Stress contour of the S10P flat slab model: (a) top view, (b) bottom view

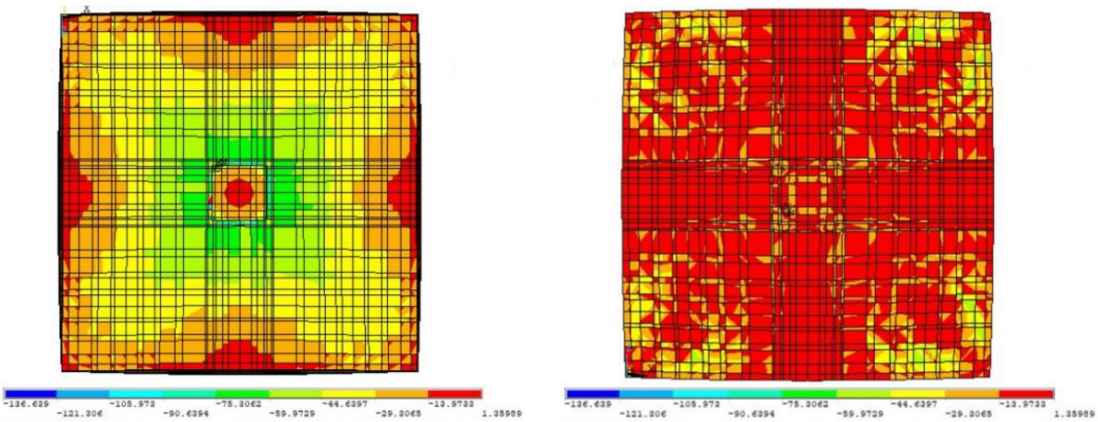

(a) (b)

Figure 12. Stress contour of the S12P flat slab model: (a) top view, (b) bottom view

4.4. Deflection contour of normal concrete flat slab

Deflection contours illustrate the deformation distribution of flat slab systems under applied loading and provide insight into the overall structural response. In all models, the maximum deflection occurs at the slab mid-span near the slab–column connection region, while deflection gradually decreases toward the supports due to boundary restraint conditions. The magnitude of deflection is governed by structural stiffness, load magnitude, and the effectiveness of shear reinforcement in controlling deformation and crack propagation.

For the unreinforced S0N model (Figure 13a), subjected to a maximum load of 321.2 kN, the maximum deflection reaches 3.16181 mm, with a minimum deflection of 0.142901 mm. The absence of shear reinforcement results in lower stiffness and reduced resistance to shear-induced deformation, leading to greater localized deflection around the column. In the S8N model (Figure 13b), subjected to a higher maximum load of 345.9 kN, the maximum deflection slightly increases to 3.31263 mm, while the minimum deflection reaches 0.151766 mm. Although shear reinforcement improves crack control and load transfer mechanisms, the higher applied load increases overall deformation. This behavior indicates that deflection response is influenced not only by reinforcement configuration but also by the magnitude of the applied load.

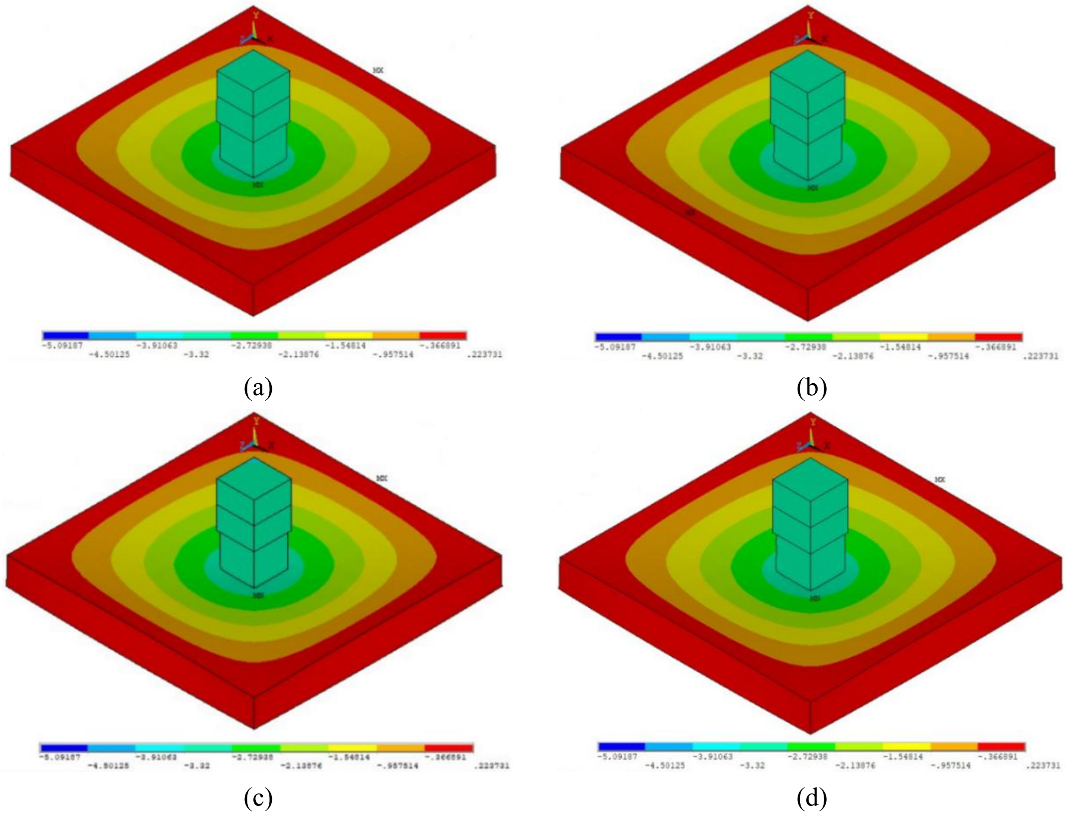

Figure 13. Deflection contours of flat slabs with normal concrete: (a) S0N model at Pmax = 321.2 kN, (b) S8N model at Pmax = 345.9 kN, (c) S10N model at Pmax = 362.5 kN, (d) S12N model at Pmax = 375 kN

Further increases in load are observed in the S10N model (Figure 13c), where a maximum load of 362.5 kN produces a maximum deflection of 3.35599 mm and a minimum deflection of 0.152699 mm. The deformation pattern remains consistent, with peak deflection concentrated around the slab–column connection region. In contrast, the S12N model (Figure 13d), subjected to the highest load of 375 kN, exhibits a slightly lower maximum deflection of 3.30849 mm and a minimum of 0.150274 mm. This reduction in deflection, despite the increased applied load, demonstrates the effectiveness of larger diameter shear reinforcement in improving structural stiffness, enhancing confinement, and controlling localized deformation around the critical punching shear zone. Quantitatively, the maximum deflection in the S12N model is approximately 1.4% lower than that of the S10N model, even under a higher loading condition.

Overall, the results indicate that deflection behavior is influenced by both the applied load level and the shear reinforcement configuration. While increasing load generally produces larger deformation, larger diameter shear reinforcement improves stiffness, enhances crack control, and limits deformation in the critical slab–column connection region. The concentration of maximum deflection at the slab mid-span confirms this region as the most critical zone governing the structural response and punching shear performance of flat slab systems (Isufi et al., 2021).

4.5. Deflection Contours of Polymer Nanocomposite Flat Slab

Deflection contours of polymer nanocomposite flat slabs illustrate the deformation behavior and structural response under monotonic loading. In all models, the maximum deflection occurs at the slab mid-span near the slab–column connection region, while deflection gradually decreases toward the supports due to boundary restraint conditions. The deformation response is governed by the applied load level, structural stiffness, and the effectiveness of shear reinforcement in controlling crack propagation and shear-induced deformation.

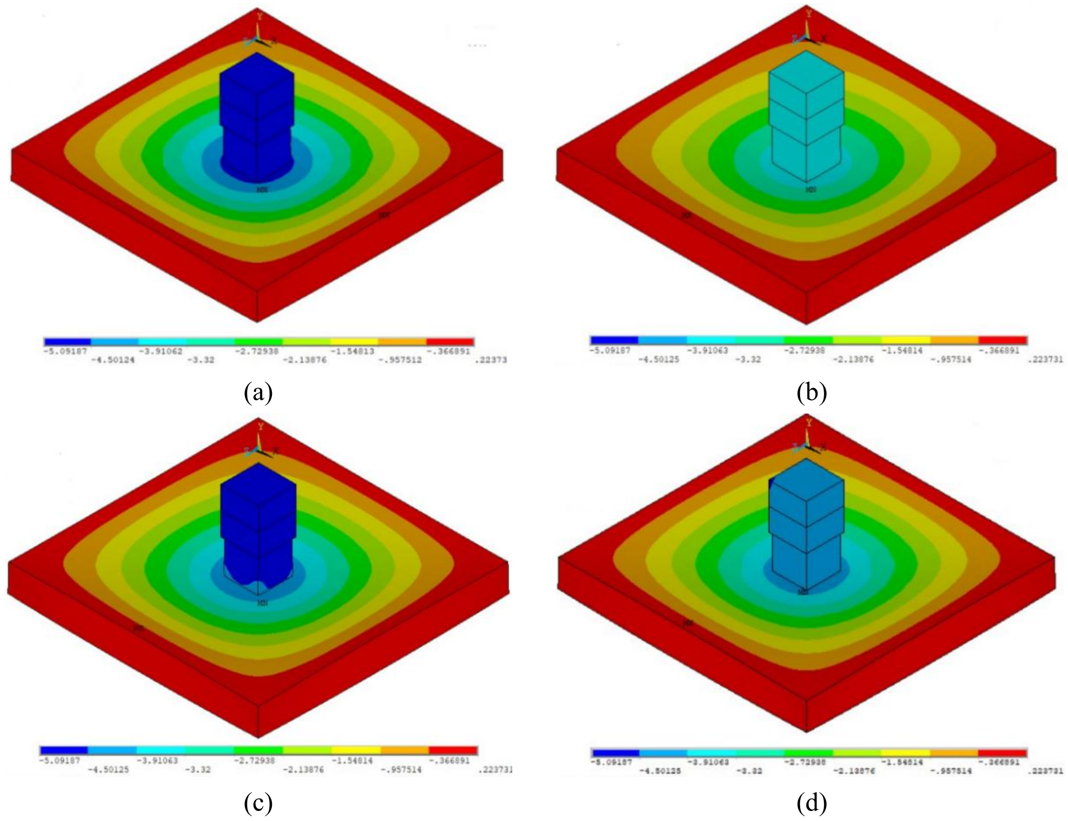

Figure 14. Deflection contours of polymer nanocomposite flat slabs: (a) S0P model at Pmax=525 kN, (b) S8P model at Pmax=537.5 kN, (c) S10P model at Pmax=550 kN (d) S12P model at Pmax=562.5 kN

The unreinforced S0P model (Figure 14a), subjected to a maximum load of 525 kN, exhibits the largest deformation with a maximum deflection of 6.3639 mm and a minimum deflection of 0.273486 mm. The absence of shear reinforcement reduces structural stiffness and confinement capacity, resulting in greater localized deformation around the column region and increased susceptibility to punching shear failure.

The introduction of shear reinforcement significantly improves deformation control. In the S8P model (Figure 14b), subjected to a load of 537.5 kN, the maximum deflection decreases to 3.94322 mm, representing a reduction of approximately 38.1% compared to the S0P model. This behavior demonstrates the effectiveness of shear reinforcement in improving stiffness, enhancing crack control, and redistributing stresses more efficiently around the slab–column connection.

For the S10P and S12P models (Figures 14c and 14d), the maximum deflections are 4.73141 mm and 4.60564 mm under loads of 550 kN and 562.5 kN, respectively. Although the applied load increases, the S12P model exhibits approximately 2.7% lower deflection than the S10P model, indicating that larger reinforcement diameters improve confinement and reduce excessive deformation around the critical punching shear zone.

Overall, the results confirm that increasing the shear reinforcement diameter improves stiffness, enhances deformation stability, and contributes to better punching shear performance in polymer nanocomposite flat slabs (Schmidt et al., 2020).

4.6. Ductility

Ductility describes how much deformation a structural member can undergo after yielding and before reaching failure. In this study, it is expressed as the ratio of ultimate to yield deflection. A larger ratio means that the slab can continue to deform after yielding and can accommodate more inelastic deformation before failure. The yield point was obtained from the load–deflection curve using a bilinear representation based on FEMA 356 (2000). The equal-area procedure was used to define the equivalent bilinear curve, so that the area represented by the idealized response remains consistent with the area of the actual load–deflection curve. The resulting yield and ultimate deflections were then used to calculate the ductility ratio for each slab model.

4.7. Ductility of Flat Slab Structures (Ewees, 2024)

The ductility values of flat slab structures obtained from two experimental models reported by Ewees (2024), with variations in shear reinforcement ratio, indicate that the highest ductility is observed in the S0N model with a value of 1.480, while the lowest ductility is recorded in the S8N model at 1.288 (Figure 15). The ductility factors obtained for both models are below 2, which places them in the low-ductility range. Interestingly, S0N gives a slightly higher ductility value than S8N, even though S0N has no shear reinforcement. This difference suggests that the deformation in S0N is influenced more by flexural behavior, whereas the addition of shear reinforcement changes how the slab transfers shear around the column. The higher ductility value of S0N should therefore not be taken to mean that the model performs better overall. Without shear reinforcement, the slab remains more vulnerable to a sudden punching shear failure, while the reinforcement in S8N provides additional resistance in the critical region.

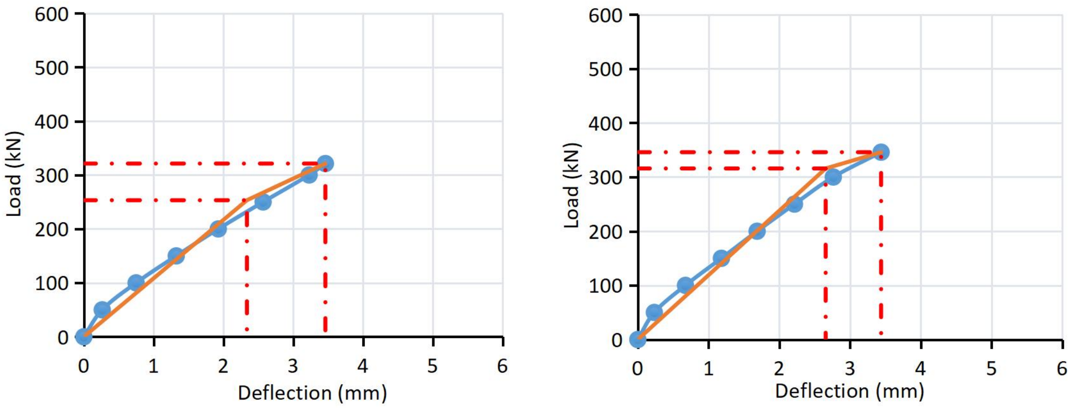

(a) (b)

Figure 15. Envelope curves for flat slab specimens: (a) S0N; (b) S8N (Ewees 2024)

4.8. Ductility of Flat Slab Structures Incorporating Normal Concrete and Polymer Nanocomposites

The ductility behavior of flat-slab structures was evaluated for both normal concrete and polymer nanocomposite materials under varying shear-reinforcement ratios. For normal concrete specimens, the ductility values are 1.510 (S0N), 1.338 (S8N), 1.311 (S10N), and 1.336 (S12N) (Figure 16). The ductility factor (μ) remains below 2 for all four models. The values are relatively close to one another, even though the amount of shear reinforcement is different. S0N gives the highest ductility value, despite having no shear reinforcement. In this case, the deformation is more closely related to the flexural response of the slab. This does not mean that S0N has better overall behavior, since the absence of shear reinforcement leaves the slab more exposed to punching failure around the column. The ductility values of S8N, S10N, and S12N are lower but remain in a similar range. The results therefore show that increasing the stirrup diameter has a limited effect on the overall ductility of the slab, while its main contribution is associated with the shear resistance of the region around the column.

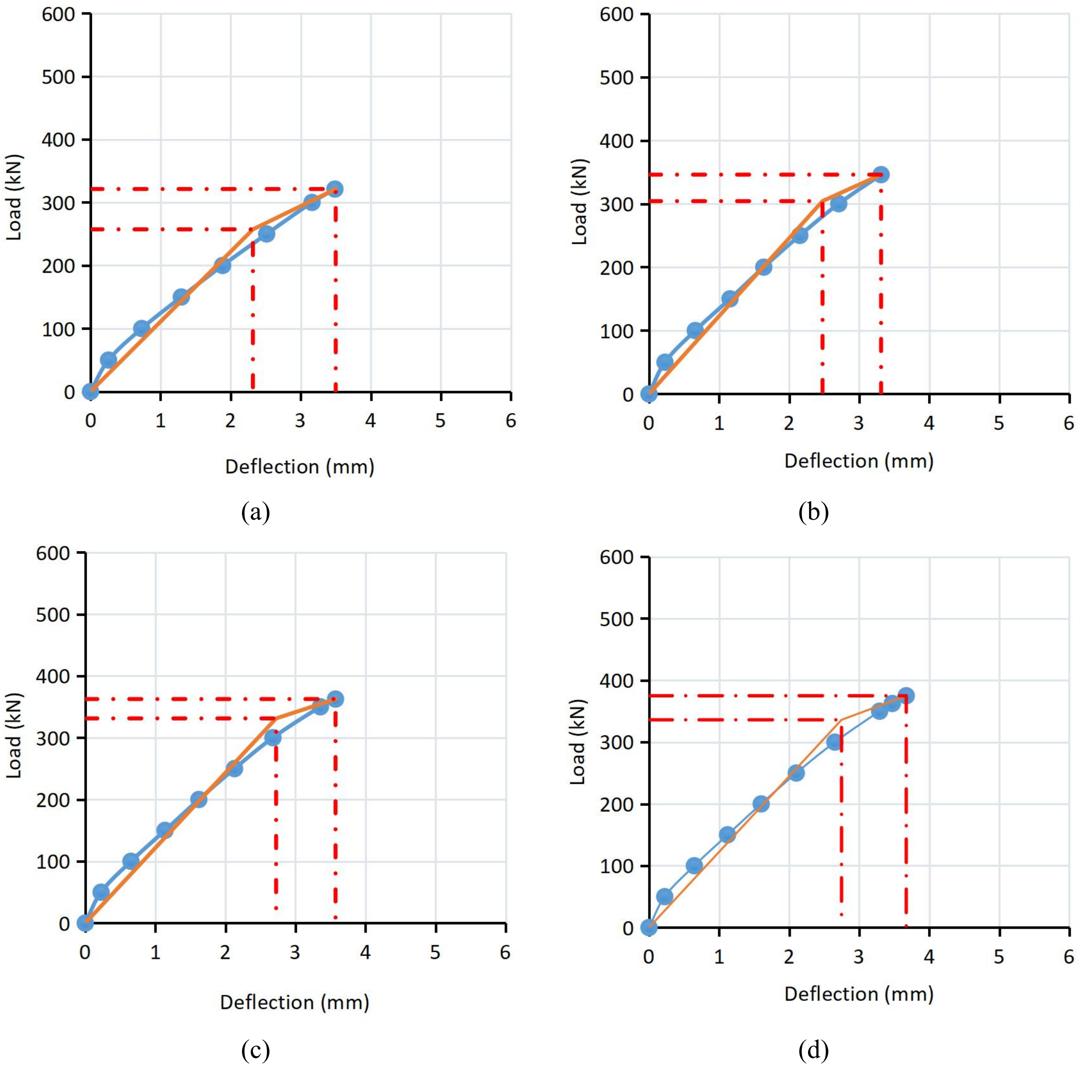

Figure 16. Envelope curves of normal concrete flat slab models: (a) S0N, (b) S8N, (c) S10N, and (d) S12N

A similar trend is observed in flat-slab structures made of polymer nanocomposite materials. The recorded ductility values are 1.749 (S0P), 1.399 (S8P), 1.482 (S10P), and 1.512 (S12P) (Figure 17), All of the models have ductility factors below 2, so they remain within the low-ductility range. S0P gives the highest value among the polymer nanocomposite models, which is consistent with the larger deformation associated with the flexural response when no shear reinforcement is provided. This higher value, however, does not mean that S0P has better structural performance. Without shear reinforcement, the slab is still more vulnerable to a sudden punching failure around the column. For the reinforced models, S8P and S10P show relatively similar ductility, while S12P gives the highest value among the three. The result suggests that increasing the stirrup diameter can provide some additional deformation capacity, although the reinforced slabs remain stiffer than S0P.

The comparison between the polymer nanocomposite and normal concrete models shows a higher ductility value for the polymer nanocomposite in every reinforcement case. S0P reaches a ductility factor of 1.749, compared with 1.510 for S0N, corresponding to an increase of about 15.8%. The difference is smaller for S8P, which increases from 1.338 in S8N to 1.399, or about 4.6%. For S10P, the value rises from 1.311 to 1.482, giving an increase of approximately 13.0%. The largest value among the reinforced cases is obtained for S12P, with a ductility factor of 1.512 compared with 1.336 for S12N, an increase of about 13.2%. Thus, the polymer nanocomposite models show a consistent increase in ductility across the reinforcement configurations considered here.

Even with these increases, the ductility values remain relatively low. The polymer nanocomposite therefore provides some improvement in deformation capacity, but this improvement does not change the overall failure behavior of the flat slab. The response is still strongly affected by punching shear around the column, which limits the amount of inelastic deformation that can develop before failure. In other words, the higher ductility obtained with the polymer nanocomposite should be viewed together with the punching shear response rather than as an indication that the slab can undergo large plastic deformation before failure.

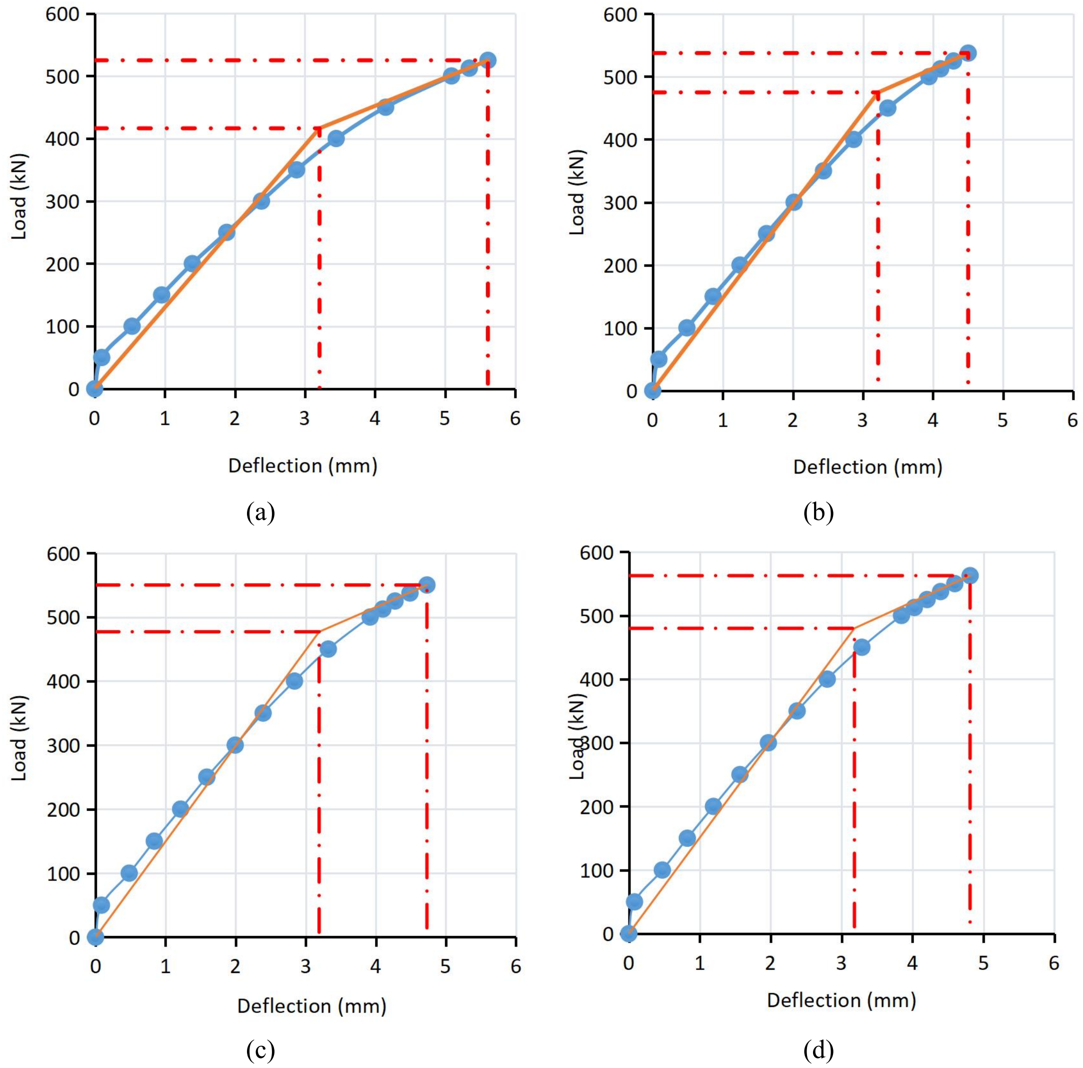

Figure 17. Envelope curves of polymer nanocomposite flat slab models: (a) S0P, (b) S8P, (c) S10P, and (d) S12P

4.9. Stiffness

Stiffness represents the ratio between the applied load and the corresponding deflection at a specific loading stage (Nurjannah et al., 2024). Figure 18 presents the stiffness response of flat slab models S0N and S8N reported by Ewees et al. (2024). The results indicate that the reinforced model (S8N) exhibits higher initial stiffness than the unreinforced model (S0N), demonstrating the contribution of shear reinforcement to improved structural rigidity and load-transfer efficiency. However, stiffness progressively decreases with increasing load due to crack initiation, propagation, and stress redistribution within the slab–column connection region. The unreinforced S0N model shows lower stiffness and reduced load-carrying capacity, making it more susceptible to punching shear failure. Figure 19 further confirms that stiffness degradation increases continuously as the applied load approaches the ultimate condition, indicating the transition from elastic to nonlinear structural behavior.

For normal concrete flat-slab models (S0N, S8N, S10N, and S12N), Figure 20 shows that stiffness decreases progressively with increasing load level. Models with shear reinforcement exhibit higher initial stiffness and slower stiffness degradation compared to the unreinforced S0N model. Among all specimens, the S12N model exhibits the highest stiffness response, indicating that increasing the diameter of the shear reinforcement improves confinement, crack control, and resistance to shear-induced deformation. In contrast, the S0N model exhibits the most significant stiffness reduction due to the absence of shear reinforcement, leading to greater crack propagation and reduced stress transfer efficiency. Figure 21 also shows that reinforced models maintain structural stiffness more effectively throughout the loading progression, confirming the important role of shear reinforcement in delaying structural degradation and improving punching shear resistance (Ewees et al., 2024; Schmidt et al., 2020; Isufi et al., 2021).

A similar trend is observed in polymer nanocomposite flat-slab models (S0P, S8P, S10P, and S12P), as shown in Figures 22 and 23. The stiffness of all models decreases as the load increases, which is expected as cracking and nonlinear deformation develop in the slab. The reinforced models start with a higher stiffness than S0P, showing the contribution of shear reinforcement to the initial response of the slab. Among the polymer nanocomposite models, S12P has the highest stiffness, while the increase in reinforcement diameter generally results in a stiffer response around the slab–column region. As loading continues, the stiffness gradually drops in all cases, although the polymer nanocomposite models maintain a more stable response than the corresponding normal concrete models. The results suggest that shear reinforcement helps the slab retain its stiffness during loading by providing additional resistance around the column and limiting the development of localized damage.

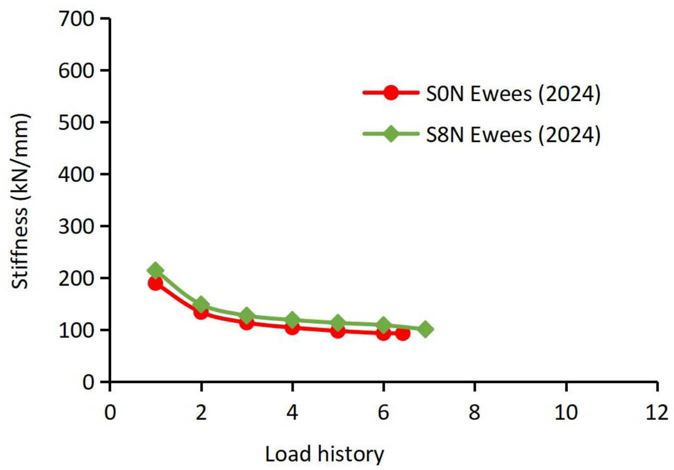

Figure 18. Stiffness response of flat slab models under progressive monotonic loading (Ewees et al. 2024)

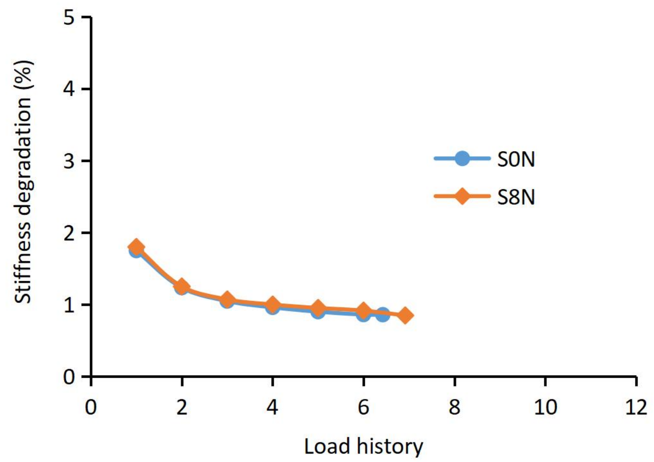

Figure 19. Stiffness degradation of flat slab models under monotonic loading (Ewees et al. 2024).

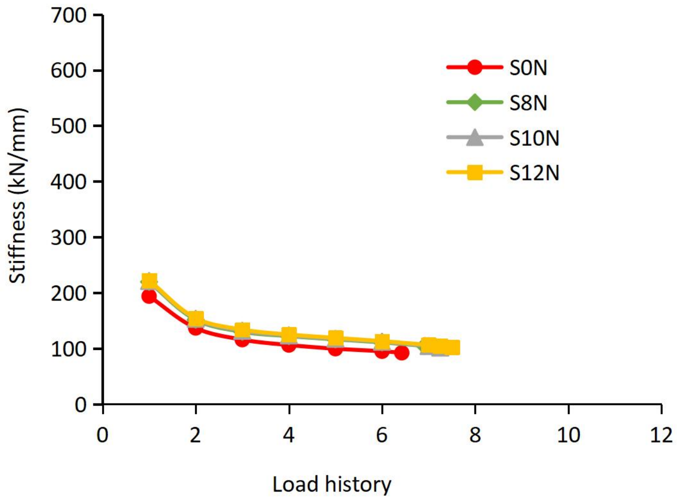

Figure 20. Stiffness response of normal concrete flat slab models under monotonic loading

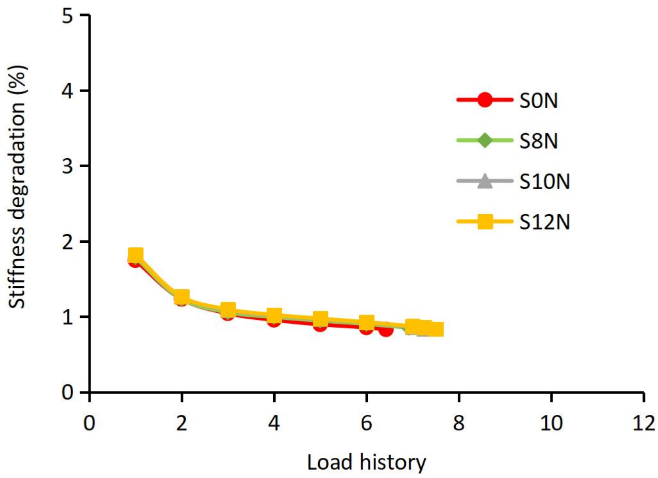

Figure 21. Stiffness degradation of normal concrete flat slab models under monotonic loading

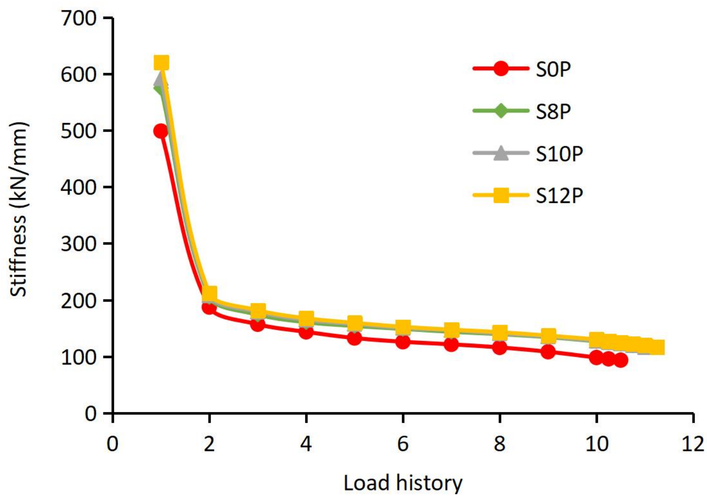

Figure 22. Stiffness degradation of polymer nanocomposite flat slab models under monotonic loading

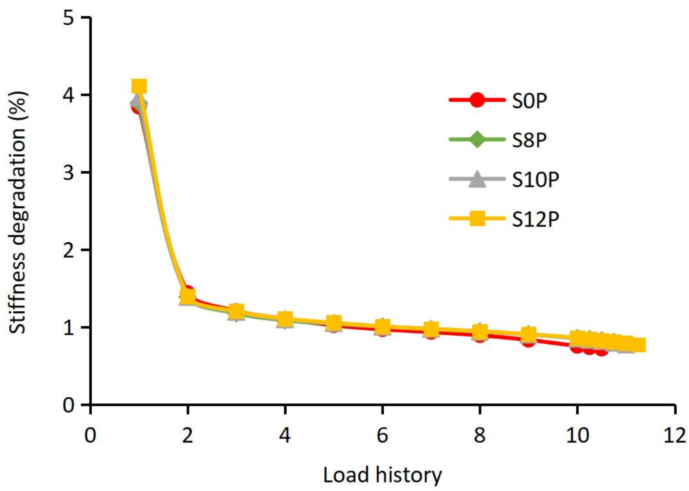

Figure 23. Stiffness degradation of polymer nanocomposite flat slab models under monotonic loading

4.10. Dissipation Energy

Energy dissipation was calculated from the area under the load–displacement curve between the yield and ultimate points. The area represents the amount of energy absorbed by the slab during the inelastic stage before failure. For the models considered here, S0N gives the largest value, at 309.01 kN·mm, whereas S8N gives the smallest value, at 250.12 kN·mm. The higher value obtained for S0N is related to its larger deformation since the model has no shear reinforcement. This produces a wider load–displacement curve and, consequently, a larger area under the curve. The lower value for S8N does not necessarily mean poorer structural behavior. The shear reinforcement changes the way the slab responds to loading and limits the deformation that develops before failure. Therefore, the higher energy dissipation of S0N needs to be considered together with its lower resistance to punching shear, since the larger deformation is accompanied by a greater possibility of sudden punching failure around the column. Visualization of the energy dissipation area for both flat-slab models (Ewees, 2024) is shown in Figure 24.

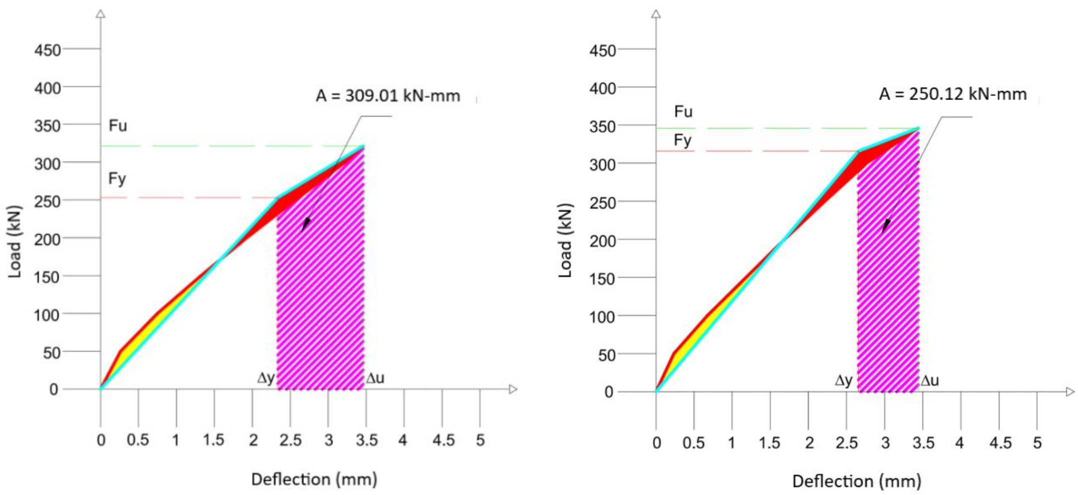

(a) (b)

Figure 24. Energy dissipation for flat slab models: (a) S0N; (b) S8N (Ewees 2024)

In flat-slab structures with normal concrete, the energy dissipation values are shown in Figure 25. The S0N model exhibits the highest energy dissipation at 326.85 kN·mm, while the S8N model shows the lowest at 251.71 kN·mm. This variation indicates that changes in the diameter of shear reinforcement influence the structure's ability to dissipate energy. Models with or without lower shear reinforcement capacity tend to exhibit greater deformation, resulting in a larger area under the load–displacement curve and, consequently, higher energy dissipation. However, this increased energy absorption is associated with reduced shear resistance and a higher susceptibility to brittle punching shear failure. For flat slab structures incorporating polymer nanocomposite materials, the energy dissipation values are shown in Figure 26. S0P gives the highest energy dissipation, with a value of 1105.27 kN·mm, while S8P gives the lowest value at 630.83 kN·mm. The difference is mainly reflected in the load–displacement response. S0P undergoes greater deformation, which produces a larger area under the curve and, consequently, a higher energy dissipation value. In S8P, the deformation is more limited, resulting in a smaller area. When the polymer nanocomposite models are compared with the corresponding normal concrete models, the difference is quite large. The energy dissipation of S0P is about 238% higher than S0N, while S8P is about 151% higher than S8N. These results show that the polymer nanocomposite slabs can absorb more energy before failure, particularly because they are able to sustain greater deformation. The higher values are also consistent with the better crack resistance and deformation response observed in the polymer nanocomposite models.

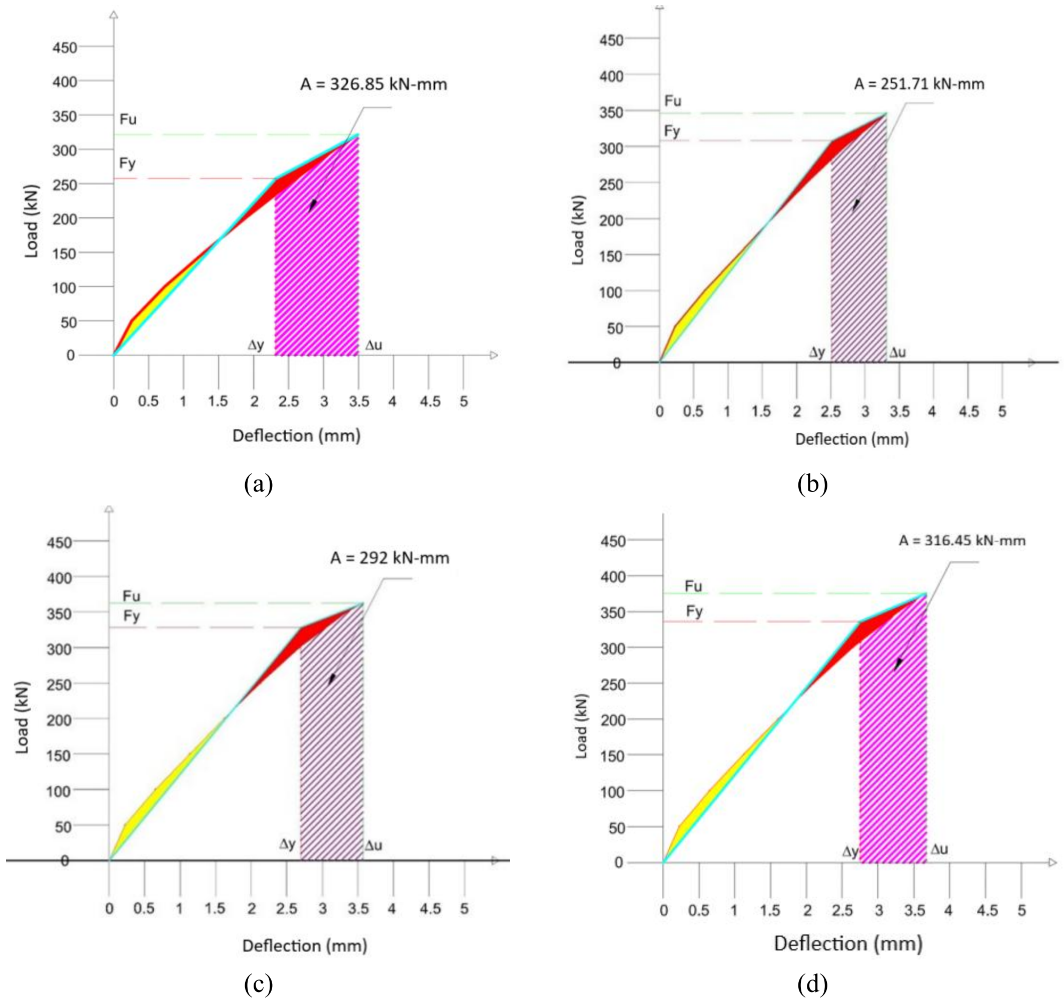

Figure 25. Energy dissipation for normal concrete specimens: (a) S0N; (b) S8N; (c) S10N; (d) S12N

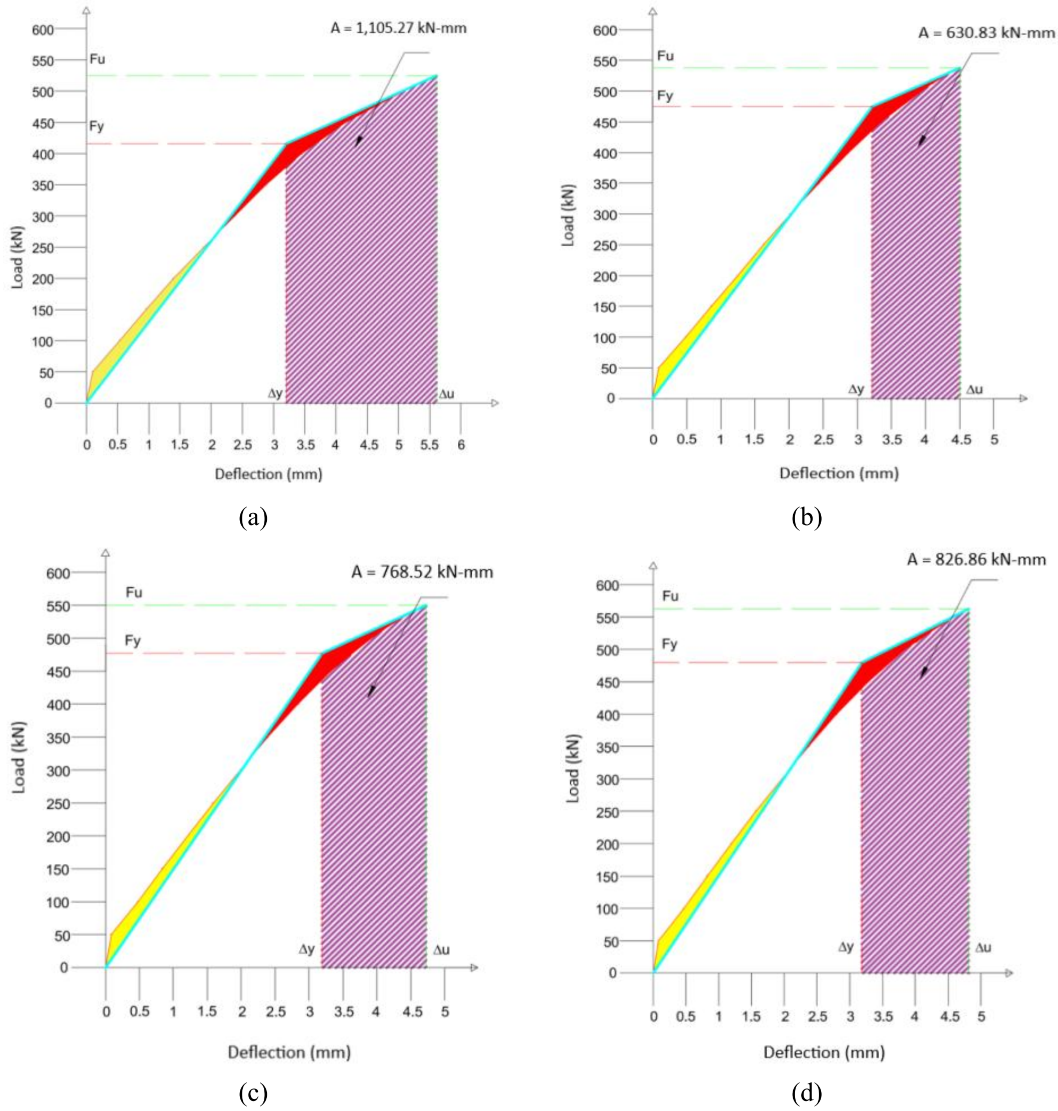

Figure 26. Energy dissipation for polymer nanocomposite specimens: (a) SOP; (b) S8P; (c) S10P; (d) S12P

4.11. Effect of Shear Reinforcement Variation on Shear Behavior

Shear force analysis of flat slab structures was conducted by comparing three modeling approaches: the model proposed by Ewees (2024), The comparison includes flat slabs made with normal concrete and those incorporating polymer nanocomposite materials. The results show that the amount of shear reinforcement affects the load that the slab can carry before punching failure. With more shear reinforcement, a larger portion of the applied load can be transferred through the slab–column region, which allows the slab to reach a higher ultimate load. The stress distribution also becomes less concentrated around the column when shear reinforcement is provided. For the S0P model, which has no shear reinforcement, failure is accompanied by concrete crushing around the column and yielding of the flexural reinforcement. The ultimate shear force reaches 262.5 kN, compared with 160.6 kN for S0N. This corresponds to an increase of about 63.4% when the normal concrete is replaced with the polymer nanocomposite material. The difference shows the contribution of the polymer nanocomposite to the shear response of the slab. Nevertheless, S0P still has no additional reinforcement to carry shear around the column, so the model remains susceptible to localized punching failure despite its higher ultimate capacity. Therefore, the incorporation of shear reinforcement remains essential for further improving shear capacity, enhancing stress distribution, and increasing overall structural reliability (Schmidt et al., 2020). The influence of shear reinforcement variation on the shear force capacity of flat slab structures is illustrated in Figure 27.

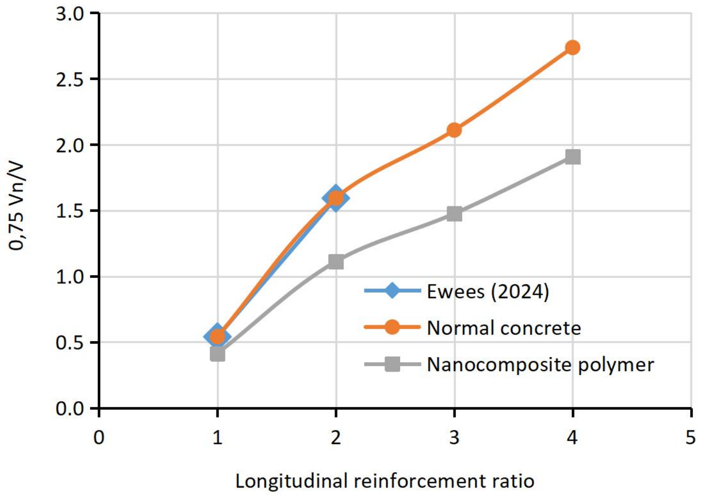

Figure 27. Effect of shear reinforcement ratio on shear capacity of flat slab models

The results show that polymer nanocomposite can be used as an option for flat slab systems where punching shear is an important concern. The effect is not only seen in the load capacity. The stress around the column is distributed differently when shear reinforcement is added, and the slabs are able to maintain their stiffness for a longer part of the loading process. The polymer nanocomposite models also show a different deformation response after cracking. At the same time, the results show that using this material by itself is not enough to determine the performance of the slab. The amount and arrangement of shear reinforcement also have a clear effect on the response. For this reason, the material properties and reinforcement details need to be considered together when the polymer nanocomposite is applied to a flat slab system.

5. Study Limitations

There are some limitations to the numerical work presented here. The slabs were analyzed only under monotonic loading, so their response under cyclic or repeated loading was not covered. The polymer nanocomposite properties were also taken from experimental data reported in previous work because no additional material or slab tests were carried out as part of this study. In the finite element model, the reinforcement was assumed to have a perfect bond with the concrete. This means that possible slip between the two materials was not captured. The model also did not include a detailed fracture-based constitutive law, which may affect the way local cracking and failure are represented. Experimental testing of the polymer nanocomposite slabs would be useful for checking these numerical results. Future work could also look at cyclic loading, bond–slip behavior, and a more detailed material model to obtain a closer representation of the failure process.

6. Conclusion

This study evaluated the structural performance of flat-slab systems using normal concrete and polymer nanocomposite materials under varying shear-reinforcement ratios. The numerical results show good agreement with previous findings (Ewees et al., 2024), with deflection differences of up to 10%, confirming the reliability of the analysis. The normal concrete slabs developed a more concentrated stress field near the column, and cracking was mainly observed in the same region. The polymer nanocomposite slabs behaved differently, particularly in terms of deformation. The largest deflection was obtained for S0P, which had no shear reinforcement. Without the stirrups, the slab was able to deform more before reaching failure. This was also reflected in the ductility and energy dissipation results. The polymer nanocomposite models generally gave higher values than the normal concrete models, with S0P reaching 1105.27 kN·mm in energy dissipation. The difference between the two types of slabs cannot be explained by compressive strength alone. The way stress was distributed around the column, together with the changes in stiffness and crack development, also affected the response.

The addition of shear reinforcement changed the behavior again. The reinforced slabs became stiffer and were able to carry a higher load, but they did not undergo as much deformation before failure as the unreinforced slabs. S12P gave the highest shear capacity, reaching 281.25 kN. The increase in stirrup diameter therefore helped the polymer nanocomposite slab resist punching shear. At the same time, the response near the column remained the main factor controlling failure. The interaction between the concrete and the reinforcement in this region ultimately determined how the punching failure developed.

Acknowledgment

The authors gratefully acknowledge the financial and institutional support provided by Universitas Sriwijaya for this research.

Ethical Approval

This study was conducted entirely using numerical modeling and finite element simulation. No human participants, animal subjects, clinical samples, personal data, or experimental procedures requiring ethical approval were involved. Therefore, ethical approval and informed consent were not applicable for this research.

References

Ismail El-kassas, A. Ali Bashandy, F.A. Mohamed Eied, M. Abd El-Salam Arab, Effect of fibers type on the behavior of fibrous high-strength self-compacted reinforced concrete flat slabs in punching with and without shear reinforcement, Constr. Build. Mater. 360 (2022), https://doi.org/10.1016/j.conbuildmat.2022.129625.

Raafat, A. Fawzi, H. Metawei, H. Abdalla, Assessment of stirrups in resisting punching shear in reinforced concrete flat slab, HBRC J. 17 (2021) 61–76, https://doi.org/10.1080/16874048.2021.1881422.

Torabian, B. Isufi, D. Mostofinejad, A.P. Ramos, Behavior of thin lightly reinforced flat slabs under concentric loading, Eng. Struct. 196 (2019), https://doi.org/10.1016/j.engstruct.2019.109327.

Abdul Qader S. Najmi, Razan H. Marahlah, Swimmer Bars as Shear Reinforcement in Reinforced Concrete Flat Slabs, 2015. https://www.researchgate.net/publication/277312978.

Alnemrawi, B. R., & Al-Rousan, R. Z. (2024). Numerical and analytical study on the punching shear capacity prediction for eccentrically loaded flat slabs with openings. Results in Engineering, 24. https://doi.org/10.1016/j.rineng.2024.103315

Isufi, M. Rossi, A.P. Ramos, Influence of flexural reinforcement on the seismic performance of flat slab – Column connections, Eng. Struct. 242 (2021), https:// doi.org/10.1016/j.engstruct.2021.112583

G.J. Milligan, M.A. Polak, C. Zurell, Finite element analysis of punching shear behaviour of concrete slabs supported on rectangular columns, Eng. Struct. 224 (2020), https://doi.org/10.1016/j.engstruct.2020.111189.

Guo, J., Chan, T. M., & Wang, Y. (2023). Experimental investigation on the structural performance of the high-strength ring strengthened dowel connection under monotonic load. Engineering Structures, 292. https://doi.org/10.1016/j.engstruct.2023.116423.

H. Lima, R. Palhares, G. Sales de Melo, M. Oliveira, Experimental analysis of punching shear in flat slabs with variation in the anchorage of shear reinforcement, Struct. Concr. 22 (2021) 1165–1182, https://doi.org/10.1002/suco.202000158.

H. Panahi, A.S. Genikomsou, Comparative evaluation of concrete constitutive models in non- linear finite element simulations of slabs with different flexural reinforcement ratios, Eng. Struct. 252 (2022), https://doi.org/10.1016/j.engstruct.2021.113617.

Hamoda, A., Abadel, A. A., Ahmed, M., Wang, V., Vrcelj, Z., & Liang, Q. Q. (2024). Punching shear performance of reinforced concrete slab-to-steel column connections incorporating ECC and UHPECC. Engineering Structures, 322. https://doi.org/10.1016/j.engstruct.2024.119145

M. Lapi, L. Secci, E. Teoni, A.P. Ramos, M. Orlando, A hybrid method for the calibration of finite element models of punching-shear in R/C flat slabs, Comput. Struct. 238 (2020), https://doi.org/10.1016/j.compstruc.2020.106323.

M.H. Ewees, A.S.A. Gabr, M. Rabie Farrag. Effect of tension and compression flexural reinforcement on punching shear strength of reinforced concrete flat slab. Alexandria Engineering Journal, 99 (2024) 282–302 https://doi.org/10.1016/j.aej.2024.05.019

M.M.G. Inacio, A.F.O. Almeida, D.M.V. Faria, V.J.G. Lúcio, A.P. Ramos, Punching of high strength concrete flat slabs without shear reinforcement, Eng. Struct. 103 (2015) 275–284, https://doi.org/10.1016/j.engstruct.2015.09.010.

N. Shatarat, D. Salman, Investigation of punching shear behavior of flat slabs with different types and arrangements of shear reinforcement, Case Stud. Constr. Mater. 16 (2022), https://doi.org/10.1016/j.cscm.2022.e01028.

N.D. Gouveia, M. Lapi, M. Orlando, D.M.V. Faria, A.M.P. Ramos, Experimental and theoretical evaluation of punching strength of steel fiber reinforced concrete slabs, Struct. Concr. 19 (2018) 217–229, https://doi.org/10.1002/suco.201700136.

P. Schmidt, D. Kueres, J. Hegger, Punching shear behavior of reinforced concrete flat slabs with a varying amount of shear reinforcement, Struct. Concr. 21 (2020) 235–246, https://doi.org/10.1002/suco.201900017.

R. Al-Rousan, O. Nusier, K. Abdalla, M. Alhassan, E.A. Vougioukas, A.A. Stamos, N. D. Lagaros, Cyclic Behavior of FRP Strengthened Beam-Column Joints under Various Concrete Damage Levels, Constr. Mater. 3 (2023) 38–61, https://doi.org/10.3390/constrmater3010004.

S.A.Nurjannah, Saloma, A.P. Usman, K.M. Aminuddin, M.M. Iqbal, Rifkah, Shear capacity of geopolymer concrete deep beams with variation of transverse reinforcement ratio, Civil Engineering and Architecture 12 (2024) 293–311. https://doi.org/10.13189/cea.2024.12012

Septriansyah, V., Saggaff, A., & Saloma. (2021). Characteristics of nanocomposite polymer with temperature variation and heating time by using simple mixing method. International Journal of Advanced Technology and Engineering Exploration (IJATEE), 8(78), 651–661. http://dx.doi.org/10.19101/IJATEE.2021.874037

Septriansyah, V., Saloma, Siti Aisyah Nurjannah (2025). Effect of Nanosilica Addition and Temperature on Durability of Polymer Mortar in Seawater Environment. Science and Technology Indonesia, ISSN: 25804405 Volume: 10 Issue: 3, 847 - 855. DOI: 10.26554/sti.2025.10.3.847-855.

Septriansyah, V., Saloma, Siti Aisyah Nurjannah (2025). Effect of the Nano-Silica Addition on the Mechanical Properties of Polymer Concrete. Science and Technology Indonesia, ISSN: 25804405 Volume: 10 Issue: 1 Pages: 9 - 17 DOI: 10.26554/sti.2025.10.1.9-17

T.S. Eom, J.W. Song, J.K. Song, G.S. Kang, J.K. Yoon, S.M. Kang, Punching-shear behavior of slabs with bar truss shear reinforcement on rectangular columns, Eng. Struct. 134 (2017) 390–399, https://doi.org/10.1016/j.engstruct.2016.12.048.

V. Hugo Dalosto de Oliveira, H. Jorge Nery de Lima, G. Sales Melo, Punching shear resistance of flat slabs with different types of stirrup anchorages such as shear reinforcement, Eng. Struct. 253 (2022), https://doi.org/10.1016/j.engstruct.2021.113671

W.J. Baniya, W. Zaki, C.M.R. Farrag, D.A. Rashed, Behavior of composite pre-flat slabs in resisting punching shear forces, Alex. Eng. J. 59 (2020) 333–347, https://doi.org/10.1016/j.aej.2019.12.045.